Prediction of Impact Information of Composites Laminates Considering the Practicality

Saki Hasebe[1], Ryo Higuchi[2], Tomohiro Yokozeki[3], and Shin-ichi Takeda[4]

[1,2,3]*University of Tokyo, Bunkyo-ku, Tokyo, 113-8656, Japan*
hasebe-saki866@g.ecc.u-tokyo.ac.jp
higuchi@aastr.t.u-tokyo.ac.jp
yokozeki@aastr.t.u-tokyo.ac.jp

[3] *Japan Aerospace Exploration Agency, Mitaka-shi, Tokyo, 181-0015, Japan*
takeda.shinichi@jaxa.jp

ABSTRACT

Recently, carbon fiber reinforced plastics (CFRP) have been used in various applications, including aircraft. Because they are vulnerable to out-of-plane loads, internal and external damage occurs when foreign objects impact them. Internal damage that can affect residual properties is difficult to find and judge from the outside without special devices, which are highly costed and are sometimes difficult to conduct in some locations. In this study, surface contour information was obtained from impact tests on CFRP laminates, and the predictability of compression after impact (CAI) strength was investigated using a conventional single-task random forest model, and a decision tree-based multi-task learning model with other objective variables related to impact tests. The models estimated CAI strength with around 75% R2, and the conventional single-task learning model showed the highest value. The importance of each model indicated that factors that contribute to impact-related objective variables (impactor shape, delamination area, and delamination length) and those to CAI strength do not have a strong relationship.

1. INTRODUCTION

Carbon fiber reinforced plastics (CFRP) have superior specific strength and stiffness and have been used in the aerospace industry, such as a primary structural material of Boeing 787. Various objects, such as tools, stones and hail, can collide on the aircraft surface in manufacturing, operation, and maintenance. Airline companies conduct periodic visual inspections to detect such damage, and repair the damaged structure when necessary. However, external factors easily affect visual inspections (Baaran, 2009), and the judgment of whether the structure is intact is doubtful. To address these problems, new maintenance supporting equipment has been experimentally introduced, such as a device that enables the maintenance staff to capture the surface profile of the focusing damage.

Although CFRPs are resistant to in-plane loads thanks to fibers, they are weak against out-of-plane loads. Object impact induces damage outside the surface (external damage), such as dent, matrix crack, fiber fracture, and buckling, as well as damage inside the laminate (internal damage), such as similar damage and delamination (Othman et al., 2016). External and internal damage also occur, even if the damage is barely visible (BVID, impact damage with a dent depth of 0.25-2.5 mm), which has been reported to reduce the compression after impact (CAI) strength by about 30% (Davies & Olsson, 2004).

Various experimental and analytical studies have been conducted on the CAI strength of CRRP. When specimens with low-velocity impact damage are compressed, sudden failure occurs when a particular load is reached, and CAI strength changes due to the effects of delamination and fiber buckling inside the laminates (Abir et al., 2017). While experimental and analytical studies can provide detailed analyses of damage and mechanisms for each data set, it is difficult to capture general trends because of the testing and computational costs involved.

There has been much research on predicting impact damage in CFRP using data-driven methods. One study showed that damage detection with an accuracy of 99.8% is possible using guided wave propagation in CFRP plates (Melville et al., 2018). However, in some cases, special equipment and devices are required for data acquisition, making it difficult to introduce this method into the current maintenance system.

In this study, we have examined the possibility of predicting impact object and internal damage extent from external damage profiles of CFRP plates under various impact conditions that can cause BVID (Hasebe et al., 2023). This

study focuses on CAI strength, an important indicator of aircraft durability, and verifies and discusses the predictability using a decision tree-based multi-tasking model that can consider the relevance of impact-related objective variables.

2. EXPERIMENT

2.1. Low-Velocity Impact Testing

A drop weight impact test was conducted as a low-velocity impact (LVI) test to obtain the impact damage to CFRP plates. The material used was thermoset CFRP (T800S/3900-2B, Toray), and the specimen size was 80 mm × 80 mm. The specimens were fixed with two plates that have a cutout of 60 mm × 60 mm and set with bolts at a torque of 5 kN·m.

Three parameters were utilized to simulate impacts under complex conditions: stacking sequence, impactor shape, and impact energy (Table 1, Figure 1). 422 specimens were tested in totally, and one to three specimens were used for each impact condition.

2.2. Compression After Impact Testing

After the LVI tests, a CAI test was conducted to obtain the CAI strength for the impacted CFRP laminates. This experiment conforms to JIS K 7089 reference "Method of post-impact compression test of carbon fiber reinforced plastics using small specimens." After the LVI test, both edges of the specimens were cut to the specimen size for the CAI test 80 mm × 50 mm. The experiments were conducted at a crosshead speed of 1.0 mm/min.

448 specimens, including damaged and undamaged ones from the LVI test, were utilized. In this study, the CAI strength reduction rate (the ratio of the CAI strength with damage to the compression strength without LVI damage) is used instead of the CAI strength value itself because specimens with various layers are evaluated simultaneously.

2.3. Experimental results

Figure 2 shows the relationship between CAI strength, dent depth, and delamination area. Figure 2(a) shows that, for all impactor shapes except for flat impactors, the CAI strength is distributed around 20% to 100%, independent of dent depth. The fact that clusters are generated for each impactor shape in the plots and that there is a strong correlation between dent depth and impactor shape also indicate that there is no significant relationship between dent depth and CAI strength (Hasebe et al., 2023).

On the other hand, the relationship between CAI strength and delamination area, shown in Figure-2(b), looks a negative correlation regardless of impactor shape. The larger the delamination caused by the impact, the less energy can be released during the CAI test, indicating that the CAI strength is significantly degraded. However, the data is dispersed,

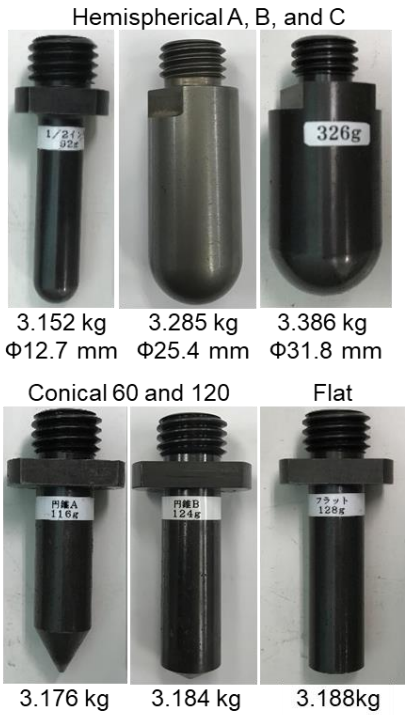

Figure 1. Impactor shape.

Table 1. Impact conditions.

Parameter	Conditions
Stacking sequence	C8 ([0/90]2s) C16 ([0/90]4s) C24 ([0/90]6s) Q8 ([45/0/-45/90]s) Q16 ([45/0/-45/90]2s) Q24 ([45/0/-45/90]3s) R0 ([0/45/0/90/0/-45/0/45/0/-45]s) R45 ([45/-45/0/45/-45/90/45/-45/45/-45]s)
Impactor shape	3 kinds of hemispherical 2 kinds of conical 1 kind of Flat
Impact energy [J/mm]	4.4, 3.35, 2.2, 1.6, 1.1

with R2 as low as 54%. Judging whether delamination area and CAI strength improve the predictability is impossible.

3. MODEL

3.1. Overview

In general machine learning, one model is usually created for each objective variable. Because it is possible to design with the most suitable hyperparameters, the model could be highly

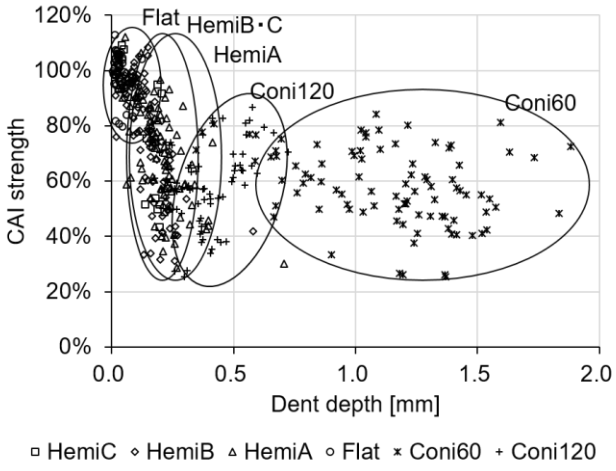

Figure 2. Dent depth vs. CAI strength.

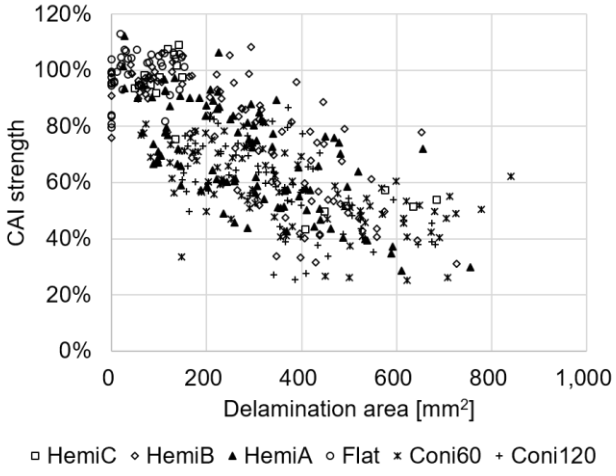

Figure 3. Delamination area vs. CAI strength.

profitable. On the other hand, such a learning model has disadvantages, such as it needs a sufficient dataset, and the relationship among objective variables cannot be considered.

This study uses decision tree-based multi-task learning to address these problems. Because it enables the prediction of multiple objective variables simultaneously, it can compensate for the shortcomings of conventional ones.

3.2. Algorithm

Figure 4 and Table 2 show the schematic structure and the hyperparameters of multi-task learning utilized in this study (Hasebe, et al., 2023). The process-by-process description of the algorithm is as follows:

1. Among the list of features, extract the defined number (*max features*) of feature names and their value to be used in the focusing branch randomly.
2. Calculate the gain, using entropy, when the sample of the parent node is divided into left and right child nodes based on a particular feature name and feature value among the candidates extracted in process #1. The entropy H_c is calculated based on the following equation for classification tasks

$$H_c = -\sum p(c|x) \log p(c|x) \quad (1)$$

where c is the class and $p(c|x)$ is the probability that class c is present at node x. On the other hand, in the case of regression tasks, considering all the data are represented by a histogram and each bin is a class,

$$H_{r|c} = \sum p(c|x) \times (-\int p(r|c,x) \log p(r|c,x)) \quad (2)$$

Using the entropy, for each objective variable (*obj*) inside the focusing node, calculate the importance (*imp*) of the parent node (*parent*) and the child node (*left*, *right*), which equals the ratio of the entropy at the focusing node to that for all samples,

$$imp_{left}^{obj} = \frac{H_{left}^{obj}}{H_{all}^{obj}} \quad (3)$$

$$imp_{right}^{obj} = \frac{H_{right}^{obj}}{H_{all}^{obj}} \quad (4)$$

$$imp_{parent}^{obj} = \frac{H_{parent}^{obj}}{H_{all}^{obj}} \quad (5)$$

The gain of the focusing node for each objective variable is then calculated from the gains when divided into each left and right child node.

$$gain_{left}^{obj} = \frac{n_{left}}{n_{parent}} \cdot (imp_{parent}^{obj} - imp_{left}^{obj}) \quad (6)$$

$$gain_{right}^{obj} = \frac{n_{right}}{n_{parent}} \cdot (imp_{parent}^{obj} - imp_{right}^{obj}) \quad (7)$$

$$gain^{obj} = gain_{left}^{obj} + gain_{right}^{obj} \quad (8)$$

Since $gain^{obj}$ is obtained for each objective variable, the average value is used as the gain of the focusing node.

$$gain = mean(gain^{obj}) \quad (9)$$

3. Process #2 should be computed for all combinations of feature names and feature values extracted in process #1. The set of the feature name and the feature value with the highest gain is used as the feature and threshold for the focusing node.
4. Repeat processes #1 through #3 to create branches. When the depth of the decision tree equals *max depth*, subsequent branches are built for each objective variable.

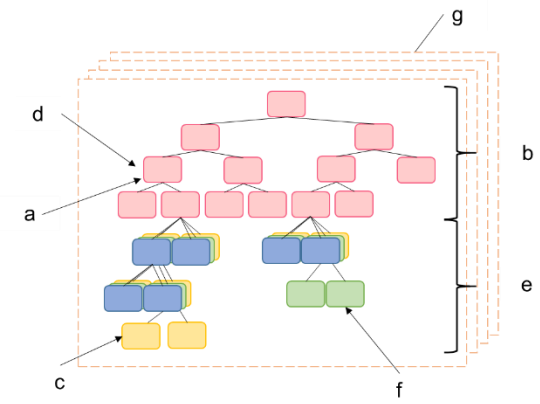

Figure 4. Multi-task learning

Table 2. Hyperparameters.

Symbol	Objective variables	Explanation
a	*Max features*	The number of features to reference in splitting an internal node
b	*Max depth*	The maximum number of layers of a common part
c	*Min samples leaf*	The minimum number of samples in leaves
d	*Min samples split*	The minimum number of samples required to split an internal node
e	*Max depth each*	The maximum number of layers of a single part
f	*Max leaf nodes*	The maximum number of leaves
g	*N estimators*	The maximum number of decision trees

5. Terminate the branch if the following conditions are met for each objective variable

- The number of samples for a parent node is less than *min samples split*
- The depth of a decision tree for each objective variable equals *max depth each*
- The number of leaves equals *max leaf nodes*
- The number of samples for a child node is less than *min samples leaf*

6. Repeat the above processes #1 through #5 to build decision trees for *n estimators*.

3.3. Feature and objective variables

The features used to train the model are those designed from surface profile data obtained from outside the specimen and those related to the specimen configuration (Hasebe, et al., 2023). A depth threshold δ (= 0.1, 0.15, 0.2, 0.25 mm) was introduced for feature engineering, to distinguish between the residual deformation of the entire plate caused by the impact test (total deformation), the local residual deformation caused by each impactor (local deformation), and the difference between total and local deformation (global deformation). For example, in the case of dent depth, the total dent depth is the depth from the reference plane of the specimen to the deepest point, while the local dent depth is the value calculated by subtracting the threshold value from the total dent depth. In the same way, several feature values were obtained: projected area of the deformed part, volume of the deformed part, and ratio of the total to the local deformation. On the other hand, the feature values related to the specimen configuration are calculated from the material constants and lamination information that can be obtained in advance, such as lamination parameters and fiber orientation information. This study utilized 155 features by using these calculation methods.

This study used four objective variables: CAI strength, delamination area, delamination length, and impactor shape category, and three patterns of objective variables were studied, as shown in Table 3. Case #1 was conducted for single-task learning with a random forest model, a conventional method. Case #2 used all objective variables for training. Case #3 was conducted to verify delamination area and length contribution to CAI strength.

4. RESULT

4.1. Prediction

Tables 3 and 4 list the results of three cases. Focusing on CAI strength, Case #1 was able to predict it in high R2 (79%). This indicates no clear relationship between CAI strength and the other objective variables. In addition, hyperparameter tuning to optimize R2 only for CAI strength was conducted as Case #2' and Case #3'. Because the learning was biased to the training data set, the model accuracy and RMSE were worse than Case #2 and #3. These results also suggest that using a multi-task learning model is inappropriate for CAI strength.

The previous study showed that for the prediction of impactor shape, delamination area, and delamination length using the multi-task learning model, the dummy objective variables that relate to the real ones, such as peak force, were effective, considering the experimental backgrounds. Because this model focused on the relationship among objective variables, it resulted in high predictability. On the other hand, because the model did not show any R2 or RMSE improvement even if it could use the other impact related objective variables, it

Table 3. Learning cases.

Case	Explanation	Objective variables
#1	Using only one target objective variable (single-task learning)	● CAI strength
#2	Using all objective variables	● CAI strength ● Delamination area ● Delamination length ● Impactor shape category
#3	Using objective variables that are not the values for LVI testing conditions	● CAI strength ● Delamination area ● Delamination length

Table 4. Learning results (regression).

Case	Objective variables	R2	RMSE
#1	CAI strength	0.785	0.097
#2	CAI strength	0.730	0.108
	Delamination area	0.666	103.924
	Delamination length	0.596	6.344
#3	CAI strength	0.755	0.103
	Delamination area	0.684	101.994
	Delamination length	0.639	5.999

Table 5. Learning results (classification).

Case	Objective variables	Accuracy	Recall
#2	Impactor shape category	0.725	0.725

indicates that the parameters that contributes to impact phenomena and CAI phenomena are different.

Comparing Case #2 and Case #3, Case#3, which does not include impactor shape as objective variable, showed better R2 and RMSE. This confirms that the impactor shape does not affect to CAI strength as shown in Figure 2.

4.2. Important feature

In Case #1, volume of high gradient area and ratio of volume is included. Volume of high gradient area gets large when the specimen has a deep local dent, or fiber breakage or cracks on the surface layer. Such dent easily causes local buckling, and fiber breakage or cracks can be a trigger of delamination development. The ratio of local to total deformation indicates that the larger the ratio is, the more the specimen has the local

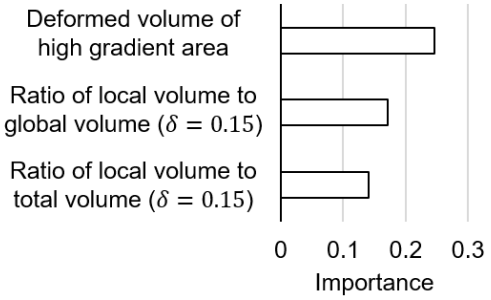

Figure 5. Top three important features (Case #1).

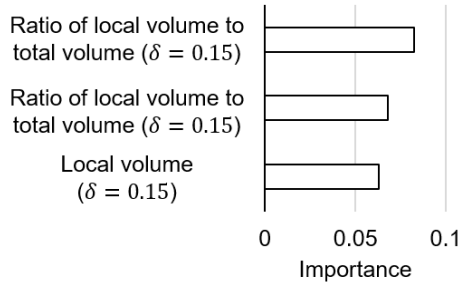

Figure 6. Top three important features of CAI strength prediction (Case #3).

deformation (deeper dent), and the smaller the ratio is, the more the specimen has residual deformation of the entire plate (shallower dent). In the CAI test, the specimen can buckle both locally and globally. Both features describe the parameters that can induce high CAI strength reduction.

Figures 5 and 6 illustrate the top three important features of Case #1 and #3. For Case #3, the ratio of deformed volume and local volume contributed to CAI strength prediction, which was the same as in Case #2. The previous study showed that dent depth and deformed local volume were important for impactor shape, delamination area and delamination length. The prediction accuracy decreased compared to the previous study, which conducted multi-task learning with multiple objective variables other than CAI strength, because the model regarded only local volume as essential.

5. CONCLUSION

This study conducted drop-weight impact and compression after impact tests on CFRP laminates to verify whether CAI strength could be predicted from external contour information on the specimens.

A conventional random forest model could predict CAI strength with 79% R2. On the other hand, the results of a multi-task learning model, which the authors proposed to improve model accuracy through synergistic effects with other objective variables (impactor shape, delamination area, and delamination length), were lower (around 75% R2). This

suggests that the parameters that contribute impact-related objective variables and those to CAI strength can differ significantly despite obtaining these values through a series of experiments in the same specimens.

In the future, this study needs to clarify the relationship between the essential features obtained in this learning and CAI strength by focusing on the CAI fracture phenomenon.

REFERENCES

Abir, MR., Tay, TE., Ridha, M., & Lee. HP. (2017). Modelling damage growth in composites subjected to impact and compression after impact. *Compos Struct*, vol.168, pp.13–25. doi: 10.1016/j.compstruct.2017.02.018

Baaran, J. (2009). *Study on Visual Inspection of Composite Structures*, EASA research project/2007/3 Final report, DTR.

Davies, GAO., & Olsson, R. (2004). Impact on composite structures. *Aeronaut J*, Vol.108, pp.541-563. doi: 10.1017/S0001924000000385.

Hasebe, S., Higuchi, R., Yokozeki, T., & Takeda S. (2023). Multi-task learning application for predicting impact damage-related information using surface profiles of CFRP laminates. *Compos Sci Technol.*, vol. 231, pp.109820. doi: 10.1017/S0001924000000385.

Melville, J., Alguri, KS., Deemer, C., & Harley, JB. (2018). Structural damage detection using deep learning of ultrasonic guided waves. *AIP Conf Proc*, 1949, pp.23004, doi: 10.1063/1.5031651

Othman, R., Ogi, K., & Yashiro, S. (2016). Characterization of microscopic damage due to low-velocity and high-velocity impact in CFRP with toughened interlayers. *Mech Eng J.*, vol.3, pp.16-00151-16-00151. doi: 10.1299/mej.16-00151

S. Hasebe was born in Tokyo, Japan. In 2020, she received her Bachelor of Aerospace Engineering from the University of Tokyo in Tokyo, Japan. In 2022, she received her Master's in Aerospace Engineering from the University of Tokyo. She is now a Ph.D. student at the University of Tokyo. She published “Internal low-velocity impact damage prediction in CFRP laminates using surface profiles and machine learning” in *Composites Part B* (doi: https://doi.org/10.1016/j.compositesb.2022.109844), and “Multi-task learning application for predicting impact damage-related information using surface profiles of CFRP laminates” in *Composites Science and Technology* (doi: https://doi.org/10.1016/j.compscitech.2022.109820) as a corresponding author. She won the Student Award from the Japan Society for Aeronautical and Space Sciences in 2020.